Contract No:

This document was prepared in conjunction with work accomplished under Contract No. 89303321CEM000080 with the U.S. Department of Energy (DOE) Office of Environmental Management (EM).

Disclaimer:

SRNL-STI-2022-609

Refrigeration system design exploration for a heavy-duty hydrogen refueling station

K. Han, PhD, PE
[Member]

B. Hardy, PhD
[Non-Member]

A. Elgowainy, PhD
[Non-Member]

K. Reddi, PhD
[Non-Member]

ABSTRACT

Due to the structural integrity of the hydrogen tank in a vehicle, high pressure hydrogen needs to be cooled down below -22°F (-30°C) before entering a dispenser and requires an efficient refrigeration system. Especially for a heavy-duty vehicle application, the design and selection of an appropriate refrigeration system is a challenging duty considering its large capacity and short charging time requirements. The purpose of this study is to design various available refrigeration systems and develop a baseline to select the most cost-effective solution. For a fixed ambient temperature and hydrogen inlet condition, diverse refrigeration systems are designed. Considered variables are the difference between the temperatures of the cold and hot streams, number of compressors, refrigerants, composition ratio of refrigerant mixtures, and refrigeration system. Several refrigeration options such as conventional vapor compression cycles, cascaded systems, auto-cascading cycles having mixed refrigerants, reverse Brayton cycles, and a vortex tube system are investigated considering the required hydrogen operating temperature. Refrigeration system characteristics are described in terms of coefficients of performance, relative heat exchanger cost, and heat exchanger size. Drawbacks and limitations of each refrigeration system are also presented.

INTRODUCTION

Global warming, which is caused by greenhouse gases such as carbon dioxide, methane, nitrous oxide, and hydrofluorocarbons is a clear and present danger to humankind. Hydrogen as an alternative vehicle motive power source draws attention to the transportation sector, which accounts for 27% of total U.S. greenhouse gas emissions (EPA 2022). Reacting hydrogen with oxygen in a fuel cell to power electric motors or burning hydrogen in an internal combustion engine are being considered because hydrogen powered vehicles have several benefits like a long range on a single refueling, no greenhouse gas emission during its consumption phase, no efficiency deterioration in cold weather, and a relatively short refuel time. On the other hand, there are many technical obstacles for hydrogen vehicles such as high carbon emission while hydrogen is being produced by steam methane reforming, expensive fuel cell catalysts, low energy content per unit volume, required energy for a hydrogen compression process, and infrastructure building encompassing production, dispensing, and transportation. Even though hydrogen has almost three times the energy content of gasoline on a mass basis, its volumetric energy density is only 25% of gasoline's. Storing hydrogen as a liquid requires cryogenic temperature below 20K. Hence, hydrogen needs to be compressed up

K. Han and **B. Hardy** are engineers at Savannah River National Laboratory, Aiken, S.C. **A. Elgowainy** is a senior scienties at Argonne National Laboratory, Lemont, IL. **K. Reddi** are a principal energy system analyst at Argonne National Laboratory, Lemont, IL.

to 700 bars for a type IV carbon-composite tank to achieve a driving range comparable to that of fossil fuel powered vehicles. Type IV vessels are intended for portable applications with light weight and are made of polymeric liner fully wrapped with a fiber-resin composite. The short refueling time requirement and high charging pressure are detrimental to the high-density polymer liner. Due to the negative Joule-Thompson coefficient of hydrogen and pressure increasement during the filling process, efficient heat removal should be accompanied. This is an especially important matter because hydrogen permeability is an exponential function of temperature and permeation not only leads to a gradual loss of hydrogen pressure, but also does damage to the reinforcement layer that can cause cyclic fatigue and mechanical failures. The typical required hydrogen temperature at the dispenser is below -22°F (-30°C) and there are several applicable refrigeration systems for the refrigeration temperature. For passenger vehicles requiring typically 200 liters of hydrogen (DOE 2017), commercialized hydrogen refueling stations are already being operated and application to heavy duty vehicles is being developed currently. For the large charging amount and short refueling time requirement, an efficient hydrogen cooling system is essential for commercial vehicle application. In this study, several refrigeration methods are evaluated in terms of thermal performance and equipment cost for the heavy-duty hydrogen refueling station. Several single-stage vapor compression cycles, cascade systems, mixed gas refrigeration systems, reverse Brayton cycles, and vortex tubes are considered as refrigeration methods to meet 10 minutes charging time at 95°F (35°C) ambient air temperature.

REFRIGERATION METHODS

It is assumed that hydrogen having 1349 lbs/hr (612 kg/h) flow rate at 104°F (40°C) and 3916 psi (27 MPa) is cooled down to -22°F (-30°C) in a precooler (evaporator) before entering a dispenser. For the selected refrigeration temperature (-22°F), the single-stage vapor compression cycle (SSVC), the cascaded cycle, and the mixed gas refrigeration (MGR) are chosen as refrigeration methods per Chakravarthy et al. (2011). COP (Coefficients of performance) is determined with the cooling load, compressor work, turbine work, and air-cooled condenser fan power. SSVC is the most widely used refrigeration method for air-conditioning and vehicles. It is composed of an evaporator, a compressor, a condenser, and an expansion device. The cascade system in this study is composed of two separate vapor compression cycles and one inter-stage heat exchanger, which is operating as an evaporator for the high temperature loop and as a condenser for the low temperature loop. MGR has been widely used in large LNG liquefaction plants. The refrigerant mixture coming out of the condenser is separated into two streams in MGR. The liquid stream is expanded and works as the low temperature fluid in the inter-stage heat exchanger. The vapor stream from the separator is cooled in the inter-stage heat exchanger and expanded before entering the evaporator. More details for MGR can be found in Chakravarthy et al. (2011). Typical process diagrams for SSVC, cascade systems, and MGR are presented in figure 1. Additionally, a reverse Brayton cycle and a vortex tube are considered. A reverse Brayton cycle is used widely in jet aircrafts as air-conditioning systems and is also utilized in the LNG industry. It is considered for the large refrigerant flow rate and turbine expansion ratio even though it is hard to justify the cost of a turbine compared to its useful work output. The vortex tube is studied in case a high-pressure gas is available at the refueling site. The vortex tube is a simple pipe that separates a compressed gas into hot and cold streams. The hot and cold streams can reach temperatures of 392°F (200°C) and -58°F (-50°C), respectively. It has no moving device and is free from Freon. All considered refrigeration systems are modeled using commercial process simulation software (2022). Heat exchanger costs are also obtained from the software. Cost information for compressors and turbines is acquired from Peters et al. (2003) and adjusted with inflation rates. Other cost factors like piping and refrigerants are not included in this study. The SRK-Twu property package (1999) is used to calculate vapor-liquid equilibrium properties (pressure, temperature, density, and compositions) and to calculate enthalpy and entropy. Compressor isentropic efficiencies are obtained from a manufacturer's open data (2022). For ammonia compressor efficiencies, the IIAR (2008) data book is used. For air compressors and turbines, 75% isentropic efficiency is assumed. For the inter-stage heat exchanger and the evaporator, a brazed plate heat exchanger is used. It should be noted that a printed circuite heat exchanger (2022) or a Packinox plate heat exchanger (2022) can handle the high-pressure hydrogen of this study. Both heat exchangers are constructed with stacking plates as the brazed plate heat exchanger. For the condenser, an air-cooled heat exchanger is chosen considering the recent environmental regulation trends for an evaporative cooling tower. Fan configuration is forced air flow. The tube has dimensions of 1" (25.4 mm) outside diameter and 2.36" (60 mm) pitch. The tube material is carbon steel. The fin tip diameter is 2.25" (57.15 mm) and the fin frequency is 11 fins per inch (433 fins per meter). The fin thickness is 0.011" (0.28 mm).

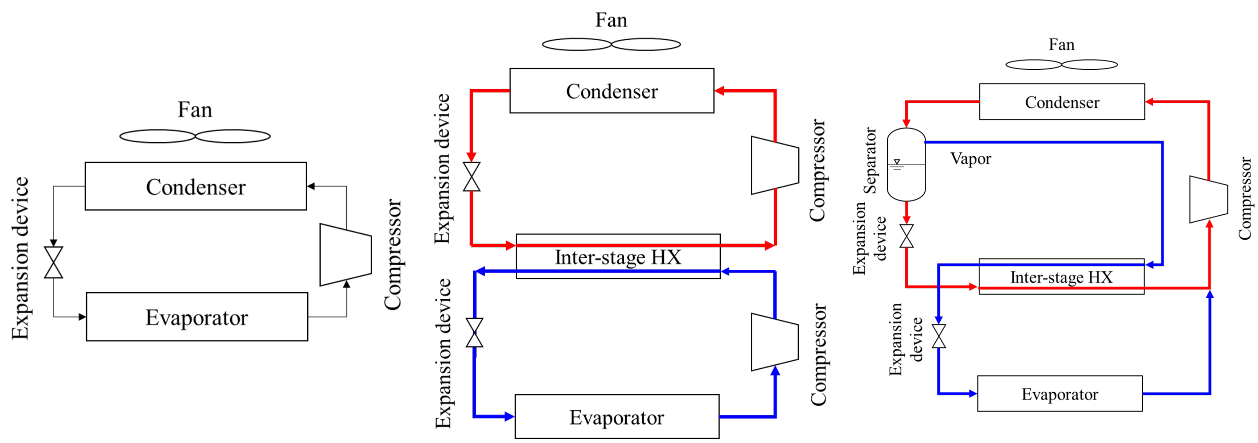

Figure 1 Process diagrams for SSVC (left), Cascaded systems (middle), and MGR (right).

RESULTS

The vapor compression cycle having a single compressor is designed at 95°F (35°C) ambient air temperature with varying refrigerant, saturated evaporating temperature (default is -31°F), and saturated condensing temperature (default is 113°F). The temperature difference between the hot and cold streams in an air-cooled condenser is 18°F (10K). For the plate heat exchanger, the temperature difference can be reduced and 9°F (5 K) is imposed in this study. The required refrigerant mass flow rate is determined using hydrogen's inlet temperature, hydrogen's inlet pressure, hydrogen's outlet temperature, refrigerant's saturated evaporation temperature, refrigerant's vapor quality at the evaporator inlet, and the refrigerant side's superheat (7.2°F). Refrigerant vapor quality is determined by the saturated condensation temperature and subcooling (7.2°F). Superheat is necessary to protect compressors from liquid slugging and subcooling is essential to prevent choked flow, vapor lock, flashing, and instability. Refrigerant and hydrogen side pressure drops are obtained with commercial heat exchanger design software (2022). The table below summarizes the operating condition, coefficient of performance, and relative cost information compared to case 1 for SSVC. Case 1 is used as a baseline. Considering the large plot area requirement, the relative air-cooled condenser plot size compared to case 1 is also included in the table. The compressor type is assumed as helical screw. Cases 1, 2, and 3 show the impact of evaporation temperature. As the evaporation temperature decreases, the compressor power increases due to the compression ratio rising. This leads to COP reduction. On the other hand, the condensation temperature reduction augments COP by decreasing the compressor work. However, the condenser's cost and its plot area significantly increase with decreasing condensing temperatures as cases 1, 4, and 5 illustrate. R507a refrigerant shows a slightly lower COP and almost the same total cost as case 1 while R134a shows a poor COP and higher cost. Ammonia shows a comparable COP and lower cost to case 1 due to its low refrigerant flow rate even though its air-cooled condenser plot size is bigger. Using cases 1 and 8, refrigerant mass flow rate impact is investigated without fixing the superheat. Cases 1 and 8 show the opposite behavior as refrigerant mass flow rate. The ammonia cycle allows a narrow refrigerant mass flow rate range.

Table 1. SSVC performance

Case	1	2	3	4	5	6	7	8
Refrigerant	R404a	R404a	R404a	R404a	R404a	R507a	R134a	Ammonia
m_{ref}	7182	7520	7806	7182	7182	7616	5353	604
e_c	66.4	67	64.8	67.5	65.7	67.8	49.9	55.3
PWR_c	165	190	217	154	174	165	201	156
PWR_f	24.8	25.3	27.2	13.6	24.9	32.6	35.4	35.4
T_e	-35	-40	-45	-35	-35	-35	-35	-35
T_c	45	45	45	40	50	45	45	45
CR	13.13	17.30	20.73	11.57	14.73	12.92	21.76	20.90
COP	0.92	0.81	0.72	1.04	0.88	0.88	0.74	0.92
A	1.00	0.99	1.05	1.99	0.88	1.21	1.22	1.18
C_{evap}	1.00	1.04	1.79	1.00	1.00	1.00	2.10	0.50
C_{cond}	1.00	1.03	1.06	2.82	0.82	1.07	1.09	1.09
C_{comp}	1.00	1.33	1.69	1.00	1.00	1.00	2.14	0.92
C_{total}	1.00	1.21	1.60	1.31	0.97	1.01	1.95	0.84

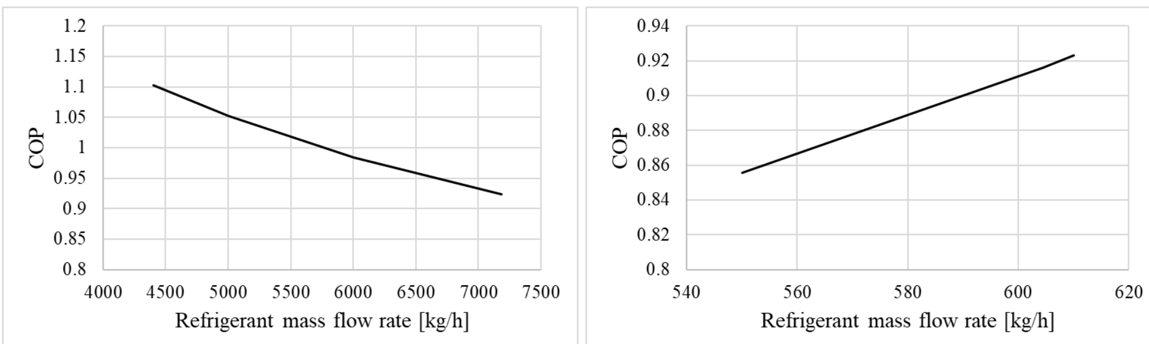

Figure 2 Refrigerant mass flow rate impacts on COP for cases 1 (left) and case 8 (right).

Cascade refrigeration systems are designed in the same way as SSVC with the saturated evaporation temperature in the inter-stage heat exchanger. Five cascade cycles are designed with varying refrigerant combination and evaporation temperatures in the inter-stage heat exchanger. For case 9, the compression ratios of the higher temperature loop and the lower temperature loop are matched to maximize COP. It gives 21.6°F(-5.76°C) for the saturated evaporation temperature in the inter-stage heat exchanger. Relative costs are also compared to case 1. Among the considered refrigerant combinations, Ammonia-CO_2 shows the best performance and the least cost. Cases 10, 11, and 12 show the impact of the evaporation temperatures of the high temperature refrigeration loop. As the temperature decreases, COP and cost increase. It is interesting to notice that the total costs of the considered cascade systems are lower than the least expensive SSVC. This is caused by the evaporator cost of the cascade system. Even though the cooling load is identical, the entering vapor quality for the cascade system is lower than SSVC because the subcooling in the condenser (inter-stage heat exchanger for the cascade system) is fixed as 7.2°F (4K). For the inter-stage heat exchanger, the condensing pressure is lower than that of SSVC. Hence, the evaporator inlet vapor quality of the cascade system is lower than that of SSVC and the cascade system can utilize more latent heat. It leads to a lower refrigerant flow rate and evaporator cost reduction. Due to the high-pressure hydrogen in the evaporator, evaporator cost is a strong influential factor in the total refrigeration system. It is worth mentioning that the compressor costs for the cascade system is not far worse than SSVC even though it requires two separate compressors. It is due to the smaller refrigerant flow rate and the lower compression ratio. Like SSVC, refrigerant mass flow impact is investigated for cases 9 and 12. Similar behavior is noticed in SSVC but R404a system cannot exceed the performance of the ammonia-CO_2 system. The ammonia-CO_2 system also has the narrow refrigerant mass flow rate range like ammonia

SSVC. The highest COP of the cascade system is lower than that of SSVC in the considered cases when superheat is not fixed.

Table 2. Cascade system performance

Case	9	10	11	12	13
$Refrigerant_h$	R404a	R134a	R134a	R134a	Ammonia
$Refrigerant_l$	R404a	CO_2	CO_2	CO_2	CO_2
$m_{ref,h}$	7275	5964.84	5971	5201	761
$m_{ref,l}$	4257	2546	2738	2481	2481
$e_{c,h}$	64.2	60.5	59.7	60.2	75.6
$e_{c,l}$	52.5	67.8	67.8	66.2	66.2
$PWR_{c,h}$	101	113	107	113	86
$PWR_{c,l}$	70	61	75	56	56
PWR_f	24.3	35.8	33.5	32.2	35.6
CR_h	4.03	6.22	5.29	7.34	6.77
CR_l	4.40	3.54	4.07	3.20	3.20
T_e	-35	-35	-35	-35	-35
T_c	45	45	45	45	45
$T_{e,int}$	-5.76	-5	0	-10	-10
COP	0.90	0.83	0.81	0.87	0.98
A	0.97	1.16	1.24	1.12	1.18
C_{evap}	0.60	0.50	0.50	0.48	0.48
C_{cond}	0.97	1.04	1.08	1.00	1.04
C_{comp}	0.98	1.08	0.99	1.13	0.72
C_{total}	0.90	0.94	0.89	0.95	0.72

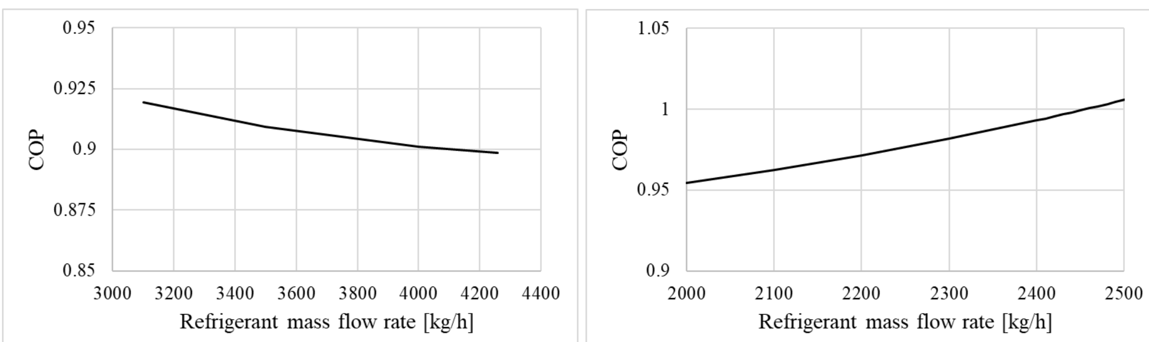

Figure 3 Refrigerant mass flow rate impacts on COP for cases 9 (left) and 13 (right).

MGR is designed with refrigerant flow rate, vapor mass fraction at the separator inlet, saturated condensing temperature (default is 113°F), saturated evaporating temperature in the evaporator (default is -31°F) and saturated evaporating temperature (default is 23°F) in the inter-stage heat exchanger. The vapor mass fraction is varied to prevent liquid slushing in the compressor and temperature cross in heat exchangers. Evaporator outlet temperature (i.e. superheat) is not fixed unlike SSVC and the cascade cycles. This enhances COP by reducing the refrigerant mass flow rate. Due to the arbitrary mixed refrigerant composition, no compressor efficiency information is available. Hence, compressor efficiency of ammonia (IIAR, 2008) is used instead. As can be found in the summary table below, the compressor efficiency for MGR is relatively higher than SSVC and the cascade cycles. Hence, COP for MGR should be interpreted carefully. Refrigerant mixture ratio is mass based.

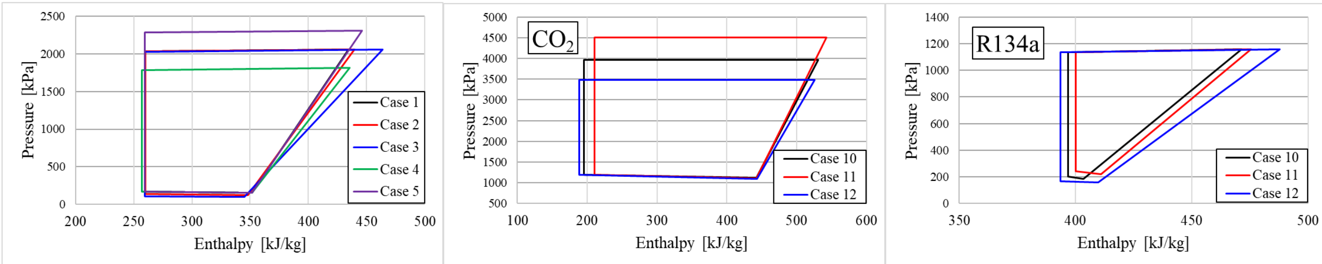

Figure 4 Pressure-Enthalpy diagrams for cases 1, 2, 3, 4, 5, 10, 11, and 12.

Cases 14, 15, and 16 are prepared to investigate the impact of saturated evaporating temperatures in the inter-stage heat exchanger. COP increases with decreasing of the temperature. Cases 17, 18, 19, and 20 are arranged to investigate the mixture composition effect. COP increases with propane mass fraction and reaches a peak at 70% mass fraction of propane. As cases 21, 22, 23, and 26 show, COP decreases with refrigerant flow rate. Cases 23, 24, and 25 provides insight into vapor mass fraction impact at the separator inlet. COP decreases with the vapor mass fraction at the separator inlet. Cases 27, 28, and 29 are prepared to explore the refrigerant combination influences. Unlike SSVC and the cascade system, ammonia only refrigerant shows a very poor performance. It is even lower than that of ammonia SSVC. Propane-CO_2 (70/30) mixture shows the highest COP among the considered MGR's, but it is lower than that of the ammonia-CO_2 cascade system and R404a SSVC with reduced refrigerant flow rate conditions. However, its total cost ratio compared to case 1 is only 0.6 which is the lowest among the considered designs. Therefore, MGR should be included as a refrigeration candidate to obtain a cost-effective solution with accurate compressor efficiency and cost data.

Table 3. MGR performance

Case	Refrigerant mixture (weight ratio)	x	m_{ref}	$T_{e,int}$	e_c	PWR_c	PWR_f	COP	A	CR
14	Propane/Ethane (70/30)	0.35	4000	-15	75.91	166	35.5	0.87	1.15	6.57
15	Propane/Ethane (70/30)	0.36	4000	-10	75.74	169	35.6	0.85	1.15	6.68
16	Propane/Ethane (70/30)	0.37	4000	-5	75.56	173	35.3	0.84	1.15	6.80
17	Propane/Ethane (80/20)	0.37	5000	-5	74.52	204	35.3	0.73	1.15	7.50
18	Propane/Ethane (40/60)	0.35	5000	-5	76.17	213	34.2	0.71	1.18	6.39
19	Propane/Ethane (50/50)	0.36	5000	-5	73.23	203	33.9	0.74	1.18	6.35
20	Propane/Ethane (70/30)	0.37	5000	-5	75.56	197	36.1	0.75	1.24	6.80
21	Propane/Ethane (60/40)	0.49	7000	-5	72.15	353	35.2	0.45	1.15	9.07
22	Propane/Ethane (60/40)	0.44	6000	-5	73.78	277	33.4	0.56	1.18	7.98
23	Propane/Ethane (60/40)	0.49	5000	-5	72.15	279	35.6	0.56	1.15	9.07
24	Propane/Ethane (60/40)	0.43	5000	-5	74.11	238	35.4	0.64	1.15	7.76
25	Propane/Ethane (60/40)	0.37	5000	-5	75.97	199	31.8	0.76	1.21	6.52
26	Propane/Ethane (60/40)	0.37	4000	-5	75.97	175	35.6	0.83	1.15	6.52
27	Propane/CO_2 (70/30)	0.41	5200	-5	77.44	157	48.0	0.85	1.06	5.55
28	R32/CO_2 (70/30)	0.41	4900	-5	72.94	209	35.1	0.72	1.18	8.54
29	Ammonia	0.71	2900	-5	57.12	682	36.0	0.24	1.18	19.07

A designed reverse Brayton cycle shows only 0.49 COP with 75% isentropic efficiency for both compressor and turbine. Air is used as a working fluid. The turbine inlet temperature and the evaporation temperature are set as 104°F (40°C) and -31°F (-35°C). Air inlet pressure to the low temperature heat exchanger is varied and compressor outlet pressure is controlled to obtain 104°F (40°C) turbine inlet temperature. COP increases with air inlet pressure to the low temperature heat exchanger as the table below shows. The cost for case 35 is 3 times more expensive compared to case 1.

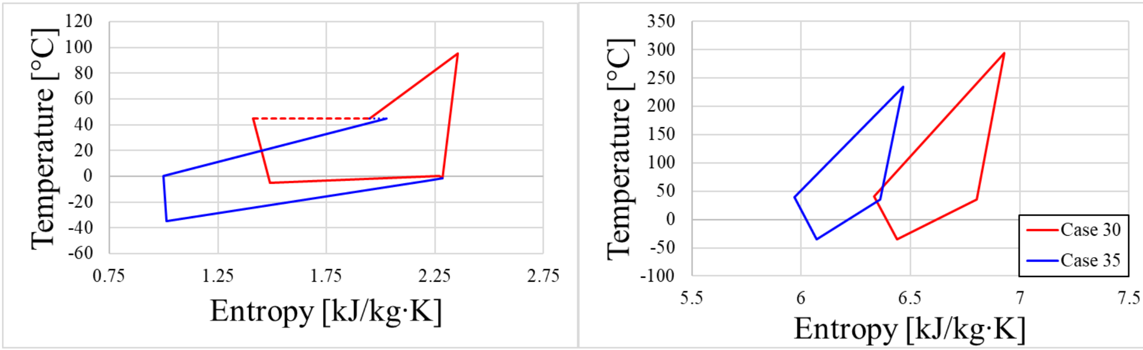

Figure 5 Temperature-Entropy diagrams for cases 27 (left), 30, and 35.

A vortex tube manufacturer (2022) claims that 126°F (70K) temperature drops with 120 psi (830 kPa) air and 25% of supplied air to a vortex tube is cooled down for the temperature drop. The required air amount for the hydrogen cooling load is 19520 lbs/hr (8854 kg/h). The cost for the precooler itself exceeds 8% of the case 1's total cost. If the compressed air is not available, it needs a compressor, a heat exchanger, and a condenser as the reverse Brayton cycle. In this case, COP is only 0.04. Hence, the vortex tube option can be considered when an ample amount of compressed gas is available at the site.

Table 4. Reverse Brayton cycle performance

Case	30	31	32	33	34	35
P	200	300	400	500	600	700
m_{ref}	9017	8995	8974	8952	8931	8910
PWR_c	663	584	548	527	514	502
PWR_t	186	183	182	180	180	178
PWR_f	34.4	35.3	34.9	34.6	34.3	34.1
CR	5.64	4.79	4.44	4.24	4.13	4.03
COP	0.34	0.40	0.44	0.46	0.48	0.49
A	1.19	1.18	1.18	1.18	1.18	1.18

CONCLUSION

A parametric study is carried out to develop a baseline for a refrigeration method that can be utilized as a heavy-duty commercial vehicle hydrogen refueling station. Various refrigeration methods such as a single-stage vapor compression cycle, a cascaded system equipped with two compressors, a mixed gas refrigeration system, a reverse Brayton cycle, and a vortex tube are evaluated in terms of system thermal efficiency, plot size, and cost. It is found that a reverse Brayton cycle is not cost-effective for this application while a vortex tube can be a good candidate if a large amount of high-pressure gas is available at the site. A cascade system and a mixed gas refrigeration cycle may save equipment cost significantly while their performances are comparable to a single-stage vapor compression system. Various design parameters such as condensing temperature, evaporation temperature, inter-stage evaporation temperature, initial temperature difference between hot and cold streams, subcooling, superheat, refrigerant, refrigerant mixture ratio, and refrigerant mass flow rate impact on the cost and the overall system performance. For the cascaded system, the ammonia-CO_2 combination is promising. The propane-CO_2 mixture shows the best performance in the considered mixed gas refrigeration systems, but it is highly recommended to search other refrigerant combinations. Finally, it should be noted that compressor efficiency and cost were estimated roughly without vendors' quotes. Detailed estimation should be discussed with equipment suppliers.

NOMENCLATURE

A	=	relative air-cooled condenser plot area compared to case 1 [-]
C_{comp}	=	relative cost of compressor compared to case 1 [-]
C_{cond}	=	relative cost of condenser compared to case 1 [-]
C_{evap}	=	relative cost of evaporator compared to case 1 [-]
C_{int}	=	relative cost of inter-cooler compared to case 1 [-]
C_{total}	=	relative cost of total system compared to case 1 [-]
COP	=	coefficient of performance [-]
CR	=	compression ratio [-]
e_c	=	isentropic compressor efficiency [-]
m_{ref}	=	refrigerant flow rate [kg/h]
P	=	air inlet pressure to heat exchanger [kPa]
PWR_c	=	compressor work [W]
PWR_f	=	fan power consumption [W]
PWR_t	=	power generation by turbine [W]
T_e	=	evaporation temperature [°C]
$T_{e,int}$	=	evaporation temperature in the inter-stage heat exchanger [°C]
T_c	=	condensing temperature [°C]
x	=	vapor mass fraction at the separator inlet [-]

Subscripts

h	=	higher temperature loop
l	=	lower temperature loop

REFERENCES

Environmental Protection Agency. 2022. Carbon Pollution from Transportation. www.epa.gov/transportation-air-pollution-and-climate-change/carbon-pollution-transportation.

Department of Energy. 2017. Hydrogen storage. www.energy.gov/sites/prod/files/2017/03/f34/fcto-h2-storage-fact-sheet.pdf.

Chakravarthy, V., Shah, R., and Venkatarathnam, G. 2011. A Review of Refrigeration Methods in the Temperature Range 4-300K. *J. Thermal Science and Engineering Application* 3:020801.1-020801.19.

Aspentech. 2022. Aspen HYSYS.

Peters, M., Timmerhaus, K., and West, R. 2003, *Plant Design and Economics for Chemical Engineers,* 5th ed. New York: McGraw-Hill.

Pasad, G., V. and Venkatarathnam, G. 1999, A method for avoiding trivial roots in isothermal flash calculations using cubic equations of state. *Ind. Engg. Chem., Res.* 38: 3530-3534.

Emerson. 2022. Copeland Online Product Information. webapps.emerson.com/online-product-information/#.

International Institute of Ammonia Refrigeration. 2008. Ammonia Data Book, 2nd ed.

Kobelco. 2022. Diffusion bonded compact heat exchanger. www.kobelco.co.jp/english/products/ecmachinery/dche/.

Alfa Laval. 2022. Packinox plate and frame heat exchanger. www.alfalaval.com/products/heat-transfer/plate-heat-exchangers/welded-plate-and-frame-heat-exchangers/packinox-plate-and-frame-heat-exchanger/.

Aspentech. 2022. Aspen EDR.

Vivek engineers. 2022. Vortex tube. www.vivekengineers.net/exair-products/spot-cooling/vortex-tubes-and-spot-cooling/vortex-tube.html.